Infrared−Vacuum Ultraviolet Pulsed Field Ionization-Photoelectron Study of $C_2H_4^+$ Using a High-Resolution Infrared Laser

Xi Xing, Beth Reed, Mi-Kyung Bahng, and C. Y. Ng*

Department of Chemistry, University of California, Davis, Davis, California 95616

Received: December 12, 2007; In Final Form: January 2, 2008

The infrared (IR)−vacuum ultraviolet (VUV)−pulsed field ionization-photoelectron (IR−VUV−PFI-PE) spectrum for $C_2H_4(\tilde{X}^1A_g, \upsilon_{11} = 1, N'_{K_a'K_c'} = 3_{03})$ in the VUV range of 83 000−84 800 cm^{-1} obtained using a single mode infrared laser revealed 24 rotationally resolved vibrational bands for the ion $C_2H_4^+(\tilde{X}^2B_{3u})$ ground state. The frequencies and symmetry of the vibrational bands thus determined, together with the anharmonic frequency predictions calculated at the CCSD(T)/aug-cc-pVQZ level, have allowed the unambiguous assignment of these vibrational bands. These bands are mostly combination bands. The measured frequencies of these bands yield the fundamental frequencies for $\upsilon_8^+ = 1103 \pm 10$ cm^{-1} and $\upsilon_{10}^+ = 813 \pm 10$ cm^{-1} of $C_2H_4^+(\tilde{X}^2B_{3u})$, which have not been determined previously. The present IR−VUV−PFI-PE study also provides truly rovibrationally selected and resolved state-to-state cross sections for the photoionization transitions $C_2H_4(\tilde{X}^1A_g; \upsilon_{11}, N'_{K_a'K_c'}) \rightarrow C_2H_4^+(\tilde{X}^2B_{3u}; \upsilon_i^+, N^+_{K_a^+K_c^+})$, where $N'_{K_a'K_c'}$ denotes the rotational level of $C_2H_4(\tilde{X}^1A_g; \upsilon_{11})$, and υ_i^+ and $N^+_{K_a^+K_c^+}$ represent the vibrational and rotational states of the cation.

I. Introduction

The supersonic molecular beam technique[1] has been widely used in photoelectron spectroscopy measurements to cool the neutral gaseous sample to reduce the rotational and vibrational temperatures.[2,3] The cooling of a polyatomic molecular sample to a few degree kelvin by supersonic beam technique has led to simplified pulsed field ionization-photoelectron (PFI-PE) spectrum, allowing the observation of rotational structures for many polyatomic species. We have shown that by IR laser excitation, a single rovibrational state can be selected for photoionization and PFI-PE studies.[4−8] From the point of view of a spectroscopic technique, the preparation of the molecule in single rotational states by infrared (IR) laser excitation is better than preparing only the lowest rotational state by cooling the molecule to near 0 K because many different rotational states can be accessed by IR laser excitation. Combining the structural and conformational selectivity of IR excitation and the detection sensitivity of VUV photoionization, the IR−VUV-photoion (IR−VUV−PI) and IR−VUV−PFI-PE methods are promising techniques for spectroscopic studies of neutrals and ions.

Nevertheless, the selection of a polyatomic species in a single rovibrational level requires the use of a high-resolution IR laser. In our previous IR−VUV−PI and IR−VUV−PFI-PE studies of CH_3I and C_2H_4,[6−8] which used an IR laser with an optical bandwidth of 0.25 cm^{-1} (full-width at half-maximum, fwhm), the preparation of a single rotational level was not completely realized. We have re-examined the IR−VUV−PI and IR−VUV-PE spectra of C_2H_4 using a single mode high-resolution IR-optical parametric oscillator (OPO) laser with a specified optical bandwidth of 0.007 cm^{-1} (fwhm). With the improved resolution of the IR laser, it is now possible to completely resolve the rotational transitions of the C−H stretching vibration bands of $C_2H_4(\tilde{X}^1A_g)$, allowing the preparation of C_2H_4 in a single rotational state for VUV−PFI-PE measurements.

As the simplest hydrocarbon with a C═C double bond, C_2H_4 and its cation $C_2H_4^+$ represent a model system for detailed experimental and theoretical investigations. Although all vibrational modes of the neutral have been accurately measured experimentally, only 4 [$\upsilon_2^+(a_g)$ (C−C stretching), $\upsilon_3^+(a_g)$ (CH_2 bending), $\upsilon_4^+(a_u)$ (C═C torsion), and $\upsilon_7^+(b_{3u})$ (CH_2 wagging)] of the 12 vibrational modes have been experimentally determined by the single-photon VUV−PFI-PE method.[9] Including the frequencies for the 2 C−H stretching vibrational modes [$\upsilon_{11}^+(b_{1u})$ and $\upsilon_{12}^+(b_{1u})$] determined in the recent IR−VUV−PFI-PE measurement,[8] 6 fundamental vibrational frequencies for $C_2H_4^+$ are now precisely measured experimentally.

As shown in the previous studies,[4−8] the IR−VUV−PFI-PE method allows the change in the symmetry of the initial neutral vibrational state, making possible the access of the ion vibrational bands that cannot be reached by the single photon VUV−PFI-PE method. We have recently improved the resolution and sensitivity of the IR−VUV-photoion and IR−VUV−PFI-PE measurements by using a newly implemented high-resolution IR-OPO laser system.[10] By employing this high-resolution IR-OPO laser system, we have re-examined the VUV−PFI-PE spectra by selecting single rotational levels ($N'_{K_a'K_c'}$) of the $C_2H_4(\upsilon_{11})$ vibrational state, aiming to observe new vibrational bands, which would lead to the determination of new fundamental vibrational frequencies of $C_2H_4^+(\tilde{X}^2B_{3u})$. The analysis of these measurements has led to truly rovibrationally selected and resolved state-to-state cross sections for the photoionization transitions, $C_2H_4(\tilde{X}^1A_g, \upsilon_{11}, N'_{K_a'K_c'}) \rightarrow C_2H_4^+(\tilde{X}^2B_{3u}; \upsilon_i^+, N^+_{K_a^+K_c^+})$, where υ_i^+ and $N^+_{K_a^+K_c^+}$ are the vibrational and rotational quantum numbers of the cation.

II. Experiment

The arrangement of the VUV laser photoion-photoelectron apparatus and procedures used for IR−VUV−PFI−PI and IR−

* To whom correspondence should be addressed. Electronic mail: cyng@chem.ucdavis.edu.

10.1021/jp711684w CCC: $40.75
Published on Web 02/20/2008

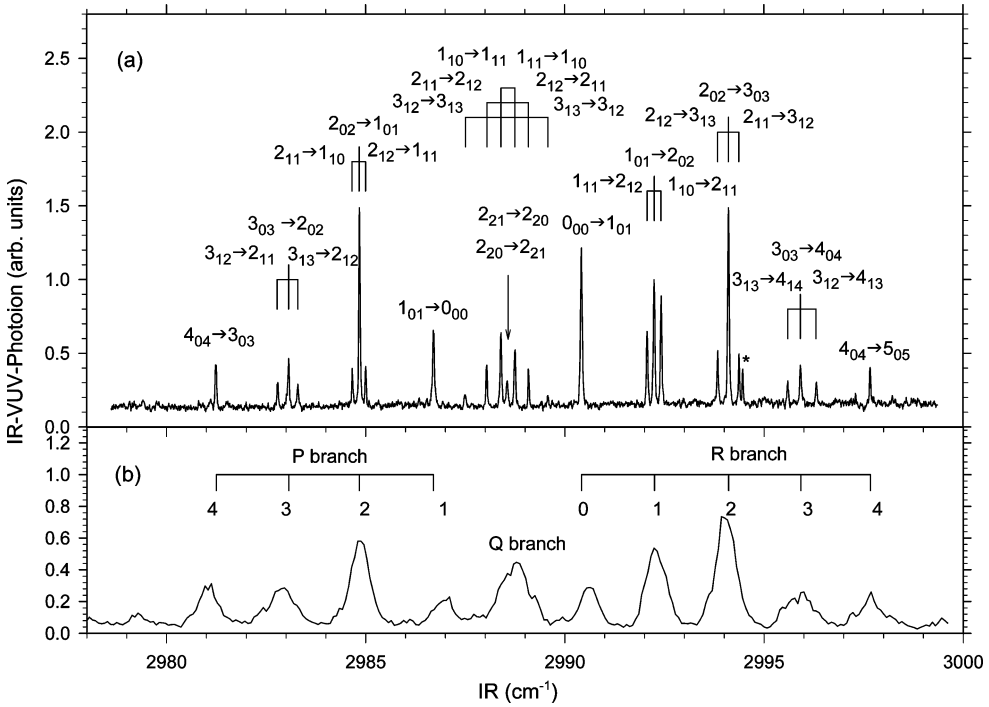

Figure 1. IR−VUV−PI spectra of C_2H_4 ($\tilde{X}^1A_g$; υ_{11}) in the IR frequency range of 2978−3000 cm^{-1} recorded by using (a) the single mode IR-OPO laser [resolution achieved = 0.02 cm^{-1} (fwhm)] and (b) the lower resolution IR-OPO laser [resolution achieved = 0.25 cm^{-1} (fwhm)]. The assignment of rotational transitions $N''_{K_a''K_c''} \rightarrow N'_{K_a'K_c'}$ are marked on top of the spectrum plotted in (a), where (N'', K_a'', K_c'') and (N', K_a', K_c') are the respective rotational quantum numbers for the ground vibrational state and the $\upsilon_{11} = 1$ excited-state of C_2H_4. The spectrum of (b) exhibits the P-, Q-, and R-branches. The assignment of the P(N''), Q(N''), and R(N'') rotational lines are marked on top of (b).

VUV−PFI-PE measurements have been described previously.[4−8,11,12] Briefly, coherent tunable VUV laser radiation was generated by four-wave difference-frequency mixings ($2\omega_1-\omega_2$) in a Kr free jet, where ω_1 and ω_2 are the UV and visible frequencies produced by two dye lasers. The UV frequency ω_1 is fixed at 49 427.53 cm^{-1} (202.316 nm) to match the two-photon resonance of the Kr transition, $(4p)^5(^2P_{1/2})5p'^1/_2(J=0) \leftarrow (4p)^6\ ^1S_0$, at 98 855.06 cm^{-1} ($=2\omega_1$). The 202.32 nm light is generated by tripling of the 606.96 nm output of a dye laser using a BBO (β-barium borate) crystal for frequency doubling followed by a KTP ($KTiOPO_4$) crystal for sum frequency mixing. The visible laser frequency ω_2 is produced by a second dye laser tunable in the range of 630−710 nm. Both dye lasers are pumped by the 532 nm output of an injection seeded Nd:YAG laser operated at 30 Hz. The VUV frequency of interest was separated from the fundamental UV and visible laser beams by a windowless VUV monochromator before entering the photoionization region of the apparatus. The optical bandwidth of the VUV radiation thus generated was measured to be 0.12 cm^{-1} (fwhm). A wavemeter was used to calibrate the wavelength of the visible laser output during the experiment. The intensities of the VUV radiation were monitored by a Cu photoelectric detector.

The IR laser system used was a single mode IR-optical parametric oscillator (IR-OPO) (Laser Vision) pumped by an injection seeded Nd:YAG laser operated at 15 Hz. The stabilization of the single mode operation was maintained by a piezo located on the rear mirror of the oscillator. The voltage on the piezo can be adjusted either manually or automatically according to the feedback from the etalon rings displayed on a monitor. This high-resolution IR-OPO laser system was tunable in the range of 1.35−5.0 μm with a specified energy resolution of 0.007 cm^{-1} (fwhm) and pulse energies in the range of 5−12 mJ. The IR pulse energies used in this study were in the range of 1−4 mJ at 3 μm, which were found to give the optimal signal-to-noise ratios. A spherical lens of 1 m focal length was used to slightly focus the IR laser beam, resulting in a spot size of ≈2 mm × 4 mm at the photoionization region.

A beam of C_2H_4 (10%) seeded in helium was produced by supersonic expansion through a pulsed valve (General valve, 30 Hz, nozzle diameter = 0.5 mm) at a stagnation pressure of 1.5 atm. The pulsed beam was skimmed by a conical skimmer before intersecting the VUV beam perpendicularly at the photoionization region, where the resulting photoions and photoelectrons were detected by an ion time-of-flight (TOF) mass spectrometer and an electron TOF spectrometer, which were equipped with microchannel plate detectors.

For IR−VUV−PI measurements,[4,8,10] the VUV frequency was fixed at 84 731 cm^{-1}, which was ≈60 cm^{-1} below the IE-(C_2H_4) = 84 790 cm^{-1}. The firing of the VUV laser is delayed by ≈100 ns with respect to the IR laser, and the IR laser frequency was scanned to record the neutral vibrational bands of interest. For IR−VUV−PFI-PE measurements, a single intermediate rovibrational state was prepared by setting the IR laser frequency at the corresponding transition and scanning the VUV laser frequency for PFI-PE measurements. The PFI-PE resolution achieved was ≈1.5 cm^{-1} (fwhm).

III. Rovibronic Assignments and Simulations

Both C_2H_4 and $C_2H_4^+$ in their ground states are considered to be planar, near-prolate asymmetric top molecule of D_{2h} symmetry. The rovibronic selection rules and their symmetry characters for IR excitation and VUV photoionization transitions from the $C_2H_4(\tilde{X}^1A_g)$ ground state have been described in detail previously and thus, will not be repeated here.[8,9]

The rotational simulations of all the observed IR−VUV−PFI-PE vibrational bands were made by calculating the rotational line positions using the rigid rotor Hamiltonians for both the neutral and ionic states:

$$H = A'^{(+)}N'_a{}^{(+)2} + B'^{(+)}N'_b{}^{(+)2} + C'^{(+)}N'_c{}^{(+)2} \qquad (1)$$

where $A'^{(+)}$, $B'^{(+)}$, and $C'^{(+)}$ denote the rotational constants of the neutral (ionic) state. The rotational levels for C_2H_4 ($C_2H_4^+$) are designated as $N'_{K_a'K_c'}$ ($N'^{+}_{K_a^{+}'K_c^{+}}$), where $N'_a{}^{(+)}$, $N'_b{}^{(+)}$, and $N'_c{}^{(+)}$ represent the total angular momentum quantum numbers without spin. The rotational constants $A' = 4.8646214(5)$ cm^{-1}, $B' = 1.00105646(11)$ cm^{-1}, and $C' = 0.82804624(13)$ cm^{-1} of neutral ethylene in the ground vibrational states were taken from ref 13. Those in the υ_{11} vibrational excited-state of neutral ethylene were taken from ref 14. The ionic rotational constants, $A^+ = 4.770(16)$ cm^{-1}, $B^+ = 0.9252(49)$ cm^{-1}, and $C^+ = 0.7832(58)$ cm^{-1} were obtained from ref 9. We have assumed that the rotational constants for all the vibrationally excited cationic states are the same as those in the vibrationless ground state of the cation. The line intensities were fitted to the spectra with a Gaussian instrumental bandwidth profile of fwhm = 1.5 cm^{-1}. The rovibronic selection rules were applied to individual vibrational bands.

IV. Results and Discussion

A. Infrared Spectra of C_2H_4 by the IR−VUV−PI Method. The IR−VUV−PI spectra of C_2H_4 were recorded by scanning the IR laser frequency in the range of 2978−3135 cm^{-1}, which covers the IR−VUV−PI vibrational bands of C_2H_4 [$\upsilon_{11}(b_{1u})$, $\upsilon_2 + \upsilon_{12}(b_{1u})$, and $\upsilon_9(b_{2u})$]. As an example, we only show the IR−VUV−PI spectrum for the C_2H_4 [$\upsilon_{11}(b_{1u})$] vibrational band in Figure 1a for comparison with that (Figure 1b) obtained previously by using a low resolution (optical bandwidth ≈0.25 cm^{-1}, fwhm) IR-OPO laser. The resolution achieved for the single mode IR−VUV−PI spectra of Figure 1a is more than 12-fold higher than that of the low-resolution spectra of Figure 1b. The larger line width observed in the IR−VUV−PI spectrum of Figure 1a than the specified optical bandwidth of the single mode IR laser may be due to the broadening effect of the photoionization process.[10]

The IR−VUV−PI spectrum of $C_2H_4(\tilde{X}^1A_g; \upsilon_{11})$ depicted in Figure 1a,b is an A-type IR transition band, where the selection rules: $\Delta N' = N' - N'' = 0, \pm 1$, $\Delta K_a' = K_a' - K_a'' = 0$ and $\Delta K_c' = K_c' - K_c'' = 1$ are valid.[15] As marked on top of Figure 1b, the low-resolution spectrum exhibits the typical P-, Q-, and R-branches.[8] The comparison of Figure 1a,b shows that the Q-branch and many of the P(N'') and R(N'') lines observed in Figure 1b consists of multiple unresolved transition lines.[8] Using the known rovibrational parameters for the υ_{11} band,[16] the energies of the allowed $N''_{K_a''K_c''} \rightarrow N'_{K_a'K_b'}$ rotational transitions are calculated and marked as downward pointing sticks on top of Figure 1a. The calculated rotational transition energies are in excellent agreement with the experimental rotational line positions. We have also simulated the rotational line intensities by taking into account the thermal distribution and the nuclear spin statistical weights of rotational levels. The simulation indicates that the rotational temperature of the C_2H_4 sample achieved in the supersonic expansion is ≈8−10 K so that more than 95% of the molecules are initially populated in rotational levels $N'' < 5$ of the ground state. For ethylene in its vibronic ground state, the nuclear spin statistical weights are 7, 3, 3, and 3 for K_aK_c = ee, eo, oe, and oo, respectively.[8,9] The largest nuclear spin statistical weight for the K_aK_c = ee levels contribute to the outstanding intensities for the transitions of $2_{02} \rightarrow 1_{01}$ in P(2), $0_{00} \rightarrow 1_{01}$ in R(0), and $2_{02} \rightarrow 3_{03}$ in R(2) as shown in Figure 1a. The peak (marked by asterisk) lying on the high-energy side of the $2_{11} \rightarrow 3_{12}$ transition is the only unassigned peak because its nature is not known.

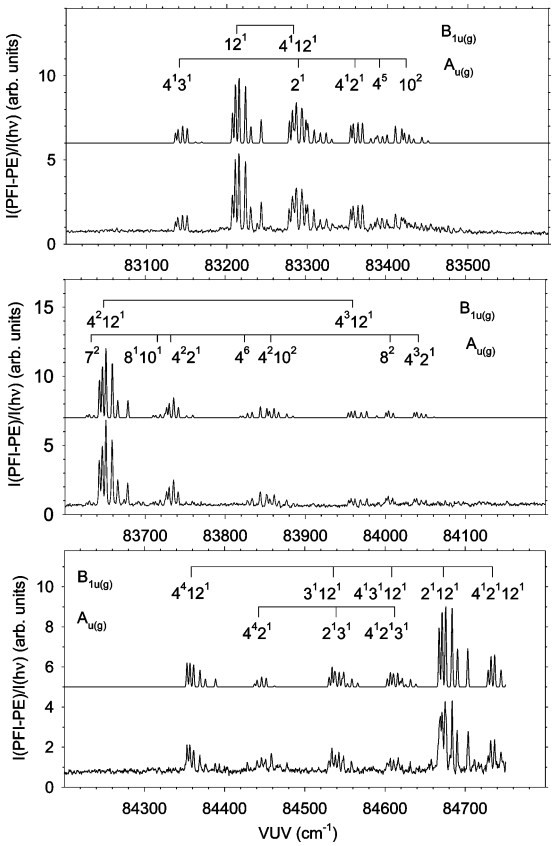

Figure 2. IR−VUV−PFI-PE spectrum of the photoionization transitions $C_2H_4(\tilde{X}^1A_g, \upsilon_{11}, N'_{K_a'K_c'} = 3_{03}) \rightarrow C_2H_4^+(\tilde{X}^2B_{3u}, \upsilon_i^+, N^+_{K_a^+K_c^+})$ in the VUV frequency ranges of (a) 83 000−83 600 cm^{-1}, (b) 83 600−84 200 cm^{-1}, and (c) 84 200−84 800 cm^{-1}. These spectra are recorded by using the single mode IR-OPO laser to select the intermediate state C_2H_4 ($\tilde{X}^1A_g$; υ_{11}, $N'_{K_a'K_c'} = 3_{03}$) via the $2_{02} \rightarrow 3_{03}$ transition. The lower curves are the experimental spectra, and the simulated spectra are shown as the upper curves. The PFI-PE intensities [I(PFI-PE)] have been normalized by the VUV intensity [$I(h\upsilon)$] and have the same units for all figures. The symmetry characters and energy position of the υ_i^+ vibrational bands of $C_2H_4^+(\tilde{X}^2B_{3u})$ are marked on the top of the simulated spectra.

B. IR−VUV−PFI-PE Spectra of C_2H_4. Figure 2a−c depict the IR−VUV−PFI-PE spectra for the ionization transitions, $C_2H_4(\tilde{X}^1A_g, \upsilon_{11} = 1, N'_{K_a'K_c'} = 3_{03}) \rightarrow C_2H_4^+(\tilde{X}^2B_{3u}, \upsilon_i^+, N^+_{K_a^+K_c^+})$ measured in the VUV frequency range of 83,000−84,800 cm^{-1}. The rovibrational level of (υ_{11}, $N'_{K_a'K_c'} = 3_{03}$)was selected by parking the IR laser frequency at the transition $2_{02} \rightarrow 3_{03}$ of R(2) as shown in Figure 1a. We note that the PFI-PE intensities [I(PFI-PE)] have been normalized by VUV intensities [$I(h\upsilon)$], and the I(PFI-PE)/$I(h\upsilon)$ units for Figure 2a−c are identical. The lower curves of these figures are the experimental spectra, and the upper curves are the simulated spectra. The assignments of the cationic vibrational bands are marked on top of the simulated spectra. Here, we use the notation υ_i^m to represent the cationic vibrational states, where m denotes the number of quanta in the vibrational mode υ_i. Knowing the IE-(C_2H_4)[8,9] = 84 790.2 cm^{-1} and $\upsilon_{11}(C_2H_4) = 2988.6$ cm^{-1},[16] it can be shown that the VUV energy range of Figure 2a−c corresponds to the total energies (the sum of IR and VUV energies) of 1200−3000 cm^{-1} above the $C_2H_4^+(\tilde{X}^2B_{3u})$ ground state.

Compared to the IR−VUV−PFI-PE spectra obtained previously using the low-resolution IR-OPO laser,[8] the current measurement is found to have a significantly higher sensitivity, allowing vibrational levels with weak intensities to be observed. Furthermore, selecting a single rovibrational level 3_{03} in the

TABLE 1: Ionization Energy (IE) Values for the Photoionization Transitions $C_2H_4(\tilde{X}^1A_g; \upsilon_{11}, N'_{K_a'K_c'}=3_{03}) \rightarrow C_2H_4^+(\tilde{X}^2B_{3u}; \upsilon_i^+)$ and Ion Vibrational Energies ($\Delta\upsilon$'s) Observed in the IR−VUV−PFI-PE Measurements (Uncertainties for IE, ±0.5 cm^{-1}; Uncertainties for $\Delta\upsilon$, ±0.2 cm^{-1})

ion vibrational band υ_i^+					
$\Gamma_\nu^+ = a_g, a_u$	$\Gamma_\nu^+ = b_{1g}, b_{1u}$	IE (cm^{-1})	$\Delta\upsilon$ (expt)[a] (cm^{-1})	$\Delta\upsilon$ (theory)[b] (cm^{-1})	$\sigma(\upsilon_{11}\rightarrow\upsilon_i^+)$[c]
3^14^1 (a_u)		83142.6	1340.8	1342 (−1)	1.6
			1340.4[e]		
	12^1 (b_{1u})	83213.7	1411.9	1413 (−1)	7.6
		83213.5[d]	1411.7[d]		
	4^112^1 (b_{1g})	83284.5	1482.7	1497 (−14)	4.4
		83284.3[d]	1482.5[d]		
2^1 (a_g)		83290.3	1488.5	1489 (1)	2.2
		83290.1[d]	1488.3[d]		
			1487.7[e]		
4^12^1 (a_u)		83360.8	1559.0	1573 (−14)	2.7
		83361.0[d]	1559.2[d]		
			1558.6[e]		
4^5(a_u)		83391.3	1589.5		1.5
			1593.6[e]		
10^2 (a_g)		83424.3	1622.5	1588 (18)	1.8
7^2 (a_g)		83633.8	1832.0	1814 (18)	<0.5
	4^212^1 (b_{1u})	83649.6	1847.8	1851 (−3)	10.0
		83650.3[d]	1848.5[d]		
8^110^1 (a_u)		83716.7	1914.9	1875 (40)	<0.5
4^22^1 (a_g)		83733.5	1931.7	1927 (5)	3.0
			1931.6[e]		
4^6(a_g)		83825.5	2023.7		<0.5
4^210^2 (a_g)		83858.5	2056.7	2026 (14)	1.5
	4^312^1 (b_{1g})	83960.5	2158.7	2178 (−19)	1.2
8^2 (a_g)		84007.3	2205.5	2162 (44)	1.0
4^32^1 (a_u)		84042.7	2240.9	2254 (−13)	0.8
	4^412^1 (b_{1u})	84359.8	2558.0	2575 (−17)	2.5
		84360.6[d]	2558.8[d]		
4^42^1 (a_g)		84443.7	2641.9	2651 (−9)	1.6
	3^112^1 (b_{1u})	84537.0	2735.2	2672 (63)	1.0
2^13^1 (a_g)		84540.5	2738.7	2748 (−9)	1.0
	$4^13^112^1$ (b_{1g})	84609.7	2807.9	2756 (52)	1.2
$4^12^13^1$ (a_u)		84613.5	2811.7	2832 (−20)	0.8
	2^112^1 (b_{1u})	84674.3	2872.5	2902 (−30)	6.0
		84690.6[d]	2872.7[d]		
	$4^12^112^1$ (b_{1g})	84735.4	2933.6	2986 (−52)	2.6

[a] $\Delta\upsilon$ values are vibrational energies for the ion vibrational states, which are determined on the basis of the IE values and the known υ_{11} value of 2988.6 cm^{-1}. [b] The theoretical CCSD(T)/aug-cc-pVQZ AH vibrational frequencies for υ_m^+, $m = 1-3$ and 5−12 of $C_2H_4^+$ (see Table 1 of ref 8), together with the experimental vibrational frequencies for $\upsilon_4^+ = 83.7$ cm^{-1}, $2\upsilon_4^+ = 438.2$ cm^{-1}, $3\upsilon_4^+ = 764.6$ cm^{-1}, $4\upsilon_4^+ = 1162.1$ cm^{-1}, and $5\upsilon_4^+ = 1593.6$ cm^{-1} of ref 9, are used to obtain the predicted $\Delta\upsilon$ values [$\Delta\upsilon$(theory)]. The values in parentheses are the deviations calculated as $\Delta\upsilon$(expt) − $\Delta\upsilon$(theory). [c] Relative cross sections for the VUV photoionization transitions $\upsilon_{11} \rightarrow \upsilon_i^+$. Here, the cross section for the strongest transition $\upsilon_{11} \rightarrow 2\upsilon_4^+ + \upsilon_{12}^+$ has been arbitrarily normalized to 10. [d] Values based on IR−VUV−PFI-PE measurements. Reference 8. [e] Values based on VUV−PFI-PE measurements. Reference 9.

present study rather than a group of three (3_{03}, 3_{13}, 3_{12}) levels in the previous measurement has resulted in simplified IR−VUV−PFI-PE spectra, making the assignment more straightforward. A total of 24 vibrational bands have been identified in the IR−VUV−PFI-PE spectra of Figure 2a−c, whereas only the 7 strongest bands have been observed in the previous IR−VUV−PFI-PE study.[8] Three of the 24 bands have also been observed in the previous single-photon VUV−PFI-PE study.[9] Taking into account the previous measurements, we conclude that 14 of the 24 bands resolved in Figure 2a−c are newly observed bands for $C_2H_4^+(\tilde{X}^2B_{3u})$. Because all these bands are completely rotationally resolved, their symmetry characters can be obtained by rotational analyses, allowing the assignment of these vibrational bands based on not only their energies but also their symmetry characters. The IE values and symmetry representations of these vibrational bands are summarized in Table 1 for comparison with the IE values and symmetry properties for the bands identified in the previous IR−VUV−PFI-PE and VUV−PFI-PE measurements.[8]

We have performed ab initio harmonic and anharmonic (AH) vibrational frequency calculations at the CCSD(T)/aug-cc-pVQZ[17] level of theory. Although nearly all the AH vibrational frequency predictions for $C_2H_4/C_2H_4^+$ are found to agree with known experimental[6,8,9,16] vibrational frequencies to better than 1%, the predicted AH frequency[8] for the υ_4^+ torsional mode is nearly 4-fold greater than the experimental[8,9] value. This indicates that it remains necessary for accurate determination of the fundamental frequencies for $C_2H_4^+$, which have not yet been measured experimentally.

In addition to the CCSD(T)/aug-cc-pVQZ AH frequencies (υ_m^+, $m = 1-3$ and 5−12), we have also used the vibrational frequencies of $\upsilon_4^+ = 83.7$ cm^{-1}, $2\upsilon_4^+ = 438.2$ cm^{-1}, $3\upsilon_4^+ = 764.6$ cm^{-1}, $4\upsilon_4^+ = 1162.1$ cm^{-1}, and $5\upsilon_4^+ = 1593.6$ cm^{-1} obtained previously by Willitsch et al.,[9] to guide the assignment of vibrational bands of $C_2H_4^+$ resolved in the IR−VUV−PFI-PE spectra of Figure 2a−c. The $\Delta\upsilon$(theory) values given in Table 1 are calculated ion vibrational energies of $C_2H_4^+$ using these experimental and theoretical vibrational frequencies, where $\Delta\upsilon$ is the energy in cm^{-1} measured with respect to the IE(C_2H_4). For combination bands, the $\Delta\upsilon$(theory) values are assumed to equal the sum of individual normal-mode frequencies. The experimental ion vibrational energies [$\Delta\upsilon$(expt)] are determined

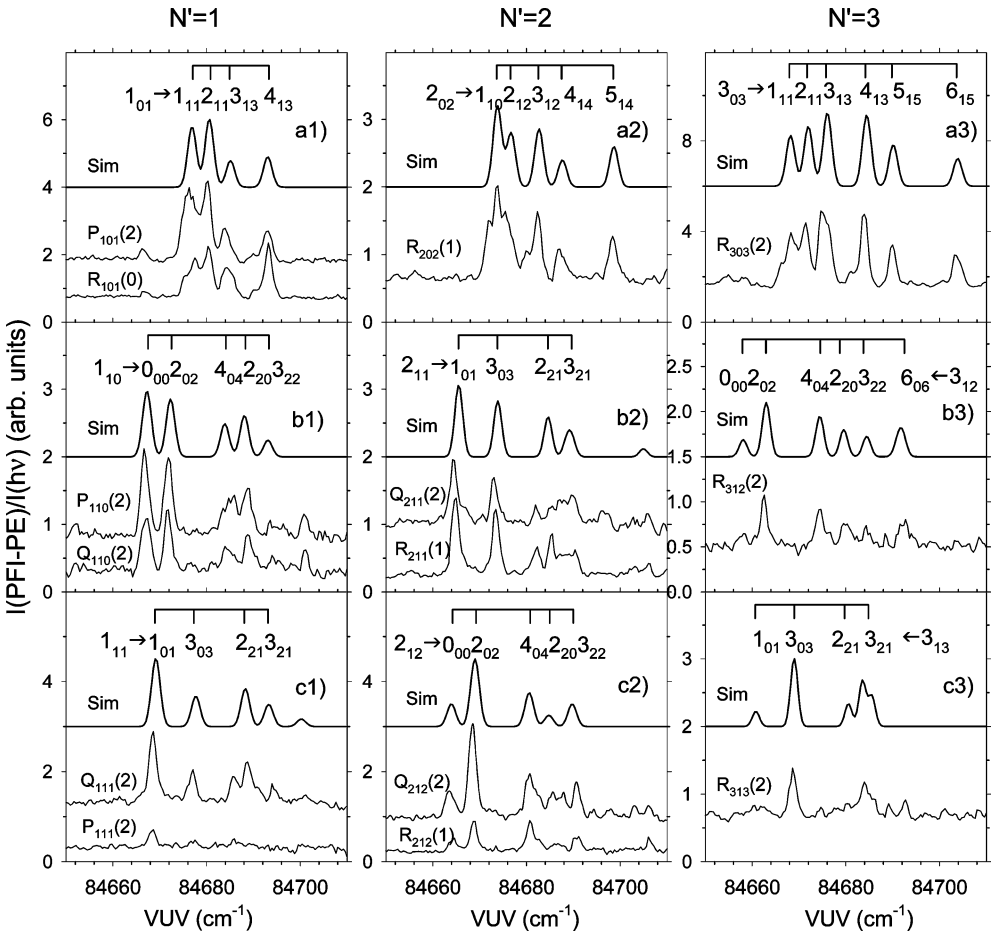

Figure 3. IR−VUV−PFI-PE spectra of the $C_2H_4(\tilde{X}^1A_g; \upsilon_{11}; N'_{K_a'K_c'}) \rightarrow C_2H_4^+(\tilde{X}^2B_{3u}; \upsilon_2^+ + \upsilon_{12}^+; N^+_{K_a^+K_c^+})$ transition in the VUV frequency range of 84 650−84 730 cm^{-1}. $N'_{K_a'K_c'} = 1_{01}$, 1_{10}, 1_{11}, 2_{02}, 2_{11}, 2_{12}, 3_{03}, 3_{12}, and 3_{13} are selected by fixing IR at different transitions (summarized in Table 2) resolved in the IR−VUV−PI spectrum of υ_{11}. The experimental spectra were shown as the middle and lower curves in a1−c1, a2−c2, a3−c3, and the simulations (sim) and assignments are shown on top of these figures. The PFI-PE intensities [I(PFI-PE)] have been normalized by the VUV intensity [$I(h\upsilon)$] and have the same units for all figures.

on the basis of the IE value for $C_2H_4(\upsilon_{11} \rightarrow \upsilon_i^+)$, the IE($C_2H_4$), and the known υ_{11} frequency of 2988.6 cm^{-1}. The deviations [$\Delta\upsilon$(expt) − $\Delta\upsilon$(theory)] are also calculated and given in parentheses in Table 1. These deviations vary in the range of 1−63 cm^{-1} and are found to be larger for higher vibrational frequencies. Because these deviations are within about 2% of the predicted frequencies,[8] we conclude that the predictions are in satisfactory agreement with experimental findings.

We found that the vibrational symmetries and rotational selection rules governing these twenty-four vibrational bands fall into two categories. The first category consists of nine vibrational bands, 4^m12^1 (m = 0, 1, 2, 3, and 4), $4^m2^112^1$ (m = 0 and 1) and $4^m3^112^1$ (m = 0 and 1), that produce the ion vibrational states of b_{1u} and b_{1g} symmetry, including the CH_2 bending mode υ_{12}^+, and its combinations with the torsional mode υ_4^+, the C−C stretching mode υ_2^+, and the CH_2 bending mode υ_3^+. The rotational selection rules governing these bands are ΔK_a = odd and ΔK_c = even, which give rise to six dominant rotational transitions, $3_{03} \rightarrow 1_{11}$ (2_{11}, 3_{13}, 4_{13}, 5_{15}, and 6_{15}), as can be seen in the pattern of the rotational structures in these bands. All the other fifteen bands, which involve the formation of ion vibrational states with a_g and a_u symmetries, are governed by the selection rules, ΔK_a = odd and ΔK_c = odd. These rules give rise to the dominant rotational transitions $3_{03} \rightarrow 1_{10}$, 2_{12}, 3_{12}, 4_{14}, 5_{14}, and 6_{16}, which are in accordance with the experimental observations. These bands comprise of mostly combination bands of ion vibrational modes υ_2^+, υ_3^+ and υ_4^+ of a_g and a_u symmetry, including the 4^m (m = 5 and 6), 4^m2^1 (m = 0, 1, 2, 3, and 4), 4^13^1, 2^13^1, and $4^12^13^1$ bands. The overtones and combination bands of $\upsilon_4^+(a_u)$, $\upsilon_7^+(b_{3u})$, $\upsilon_8^+(b_{2g})$, and $\upsilon_{10}^+(b_{2u})$, which include 4^5, 10^2, 7^2, 8^110^1, 4^6, 4^210^2, and 8^2, were also observed in the spectrum. The vibrational frequency of 1589.5 cm^{-1} for 4^5 determined here is found to be slightly lower than the value of 1593.6 cm^{-1} reported by ref 9. The vibrational frequency of 2023.7 cm^{-1} for 4^6 represents a new measurement. We found that the rotational peak between the two adjacent bands 4^5 and 10^2 (4^6 and 4^210^2) is unusually strong, indicative of significant perturbation of the two bands.

The above assignment of the combination bands shows that the vibrational frequencies of the overtones and combination bands [except the frequencies of the overtones of the υ_4^+ torsional mode] can be estimated with good precision by taking the sum of the contributing normal-mode frequencies. This, together with the observed frequencies for the 4^2 (438.2 cm^{-1}),[13] 10^2 (1622.5 cm^{-1}), and 4^210^2 (2056.7 cm^{-1}), allows us to obtain υ_{10}^+ = 810 cm^{-1}. Similarly, the observed frequency of 2205.5 cm^{-1} for the 8^2 vibrational bands gives υ_8^+ = 1103 cm^{-1}. The fact that the sum $\upsilon_8^+ + \upsilon_{10}^+$ = 1913 cm^{-1} agrees well with the measured frequency of 1914.9 cm^{-1} for the 8^110^1 vibrational band indicates that the υ_8^+ and υ_{10}^+ frequencies deduced here are highly reliable. On the basis of the discrepancies observed for υ_2^+, υ_3^+ υ_7^+, and υ_{12}^+ deduced by a similar scheme, we have assigned the uncertainty of ±10 cm^{-1} for the frequencies

deduced by this additive scheme. That is, we recommend that $\upsilon_8^+ = 1103 \pm 10$ cm^{-1} and $\upsilon_{10}^+ = 813 \pm 10$ cm^{-1}.

Because the VUV frequency was scanned continuously in the frequency range of Figure 2a−c during the IR−VUV−PFI-PE measurements, the relative PFI-PE intensities for rovibrational transitions observed can be taken as a measure of the relative cross sections for the state-to-state photoionization processes, $C_2H_4(\tilde{X}^1A_g; \upsilon_{11}, N'_{K_a'K_c'} = 3_{03}) + h\nu(\mathrm{VUV}) \rightarrow C_2H_4^+(\tilde{X}^2B_{3u}; \upsilon_i^+, N^+_{K_a^+K_c^+}) + e^-$. Among all these vibrational bands, the $4^2 12^1$ band has the strongest intensity. The relative photoionization cross sections [$\sigma(\upsilon_{11} \rightarrow \upsilon_i^+)$] given in Table 1 are based on the relative intensities of the strongest rotational transition lines of individual vibrational bands observed in Figure 2a−c. We have arbitrarily normalized the cross section value of the strongest $4^2 12^1$ band to 10. Because the pattern of rotational intensities of a vibrational band is governed by the symmetry characters of the initial neutral and final ion vibrational states, the intensity pattern of all vibrational bands with the symmetry property of $b_{1u} \rightarrow b_{1u(g)}$ are expected to be identical. The same is true for the vibrational bands with the symmetry property of $b_{1u} \rightarrow a_{u(g)}$. Thus, the relative photoionization cross sections for $\sigma(\upsilon_{11} \rightarrow \upsilon_i^+)$ given in Table 1 can easily be translated into relative photoionization cross sections for rovibrational transitions.

We note that the strongest bands observed in Figure 2a−c are 12^1, $4^2 12^1$, and $2^1 12^1$, all of which have the same symmetry as the intermediate $C_2H_4[\upsilon_{11}(b_{1u})]$ state. This is to be expected in view of the Franck−Condon consideration. The other bands, $4^4 12^1$ and $3^1 12^1$, with the b_{1u} symmetry are also found to have good intensities. For all the other bands with b_{1g}, a_u, and a_g symmetries listed in Table 1, although the transitions from υ_{11} to these bands are forbidden on the basis of FCF consideration, they are still observed with noticeable intensities. This phenomenon was also observed in other photoionization studies,[13] and can be attributed to the vibronic coupling mechanism which involves borrowing intensities from electronically excited states. However, this mechanism also has specific symmetry requirements for the coupling electronic state; and it does not apply to all the forbidden transitions observed here. Nevertheless, the symmetry restriction based on the FCF consideration is lessened when rotational and photoelectron symmetries are also considered. That is, all the ion vibrational bands identified in Figure 2a−c with the $b_{1g(u)}$ and $a_{g(u)}$ symmetries are allowed transitions based on the general rovibronic selection rules.

We have also performed detailed rotationally resolved state-to-state PFI-PE measurements of the $\upsilon_{11} \rightarrow \upsilon_2^+ + \upsilon_{12}^+$ band by using the single mode IR-OPO laser to excite single rotational levels prior to the VUV−PFI-PE measurements. Fifteen rotational transition lines, $1_{01} \rightarrow 0_{00}$ of P(1) [$P_{000}(1)$], $2_{02} \rightarrow 1_{01}$ of P(2) [$P_{101}(2)$], $0_{00} \rightarrow 1_{01}$ of R(0) [$R_{101}(0)$], $2_{12} \rightarrow 1_{10}$ of P(2) [$P_{110}(2)$], $1_{01} \rightarrow 1_{10}$ of Q(1) [$Q_{110}(1)$], $2_{12} \rightarrow 1_{11}$ P(2) [$P_{111}(2)$], $1_{10} \rightarrow 1_{11}$ of Q(1) [$Q_{111}(1)$], $1_{01} \rightarrow 2_{02}$ of R(1) [$R_{202}(1)$], $1_{10} \rightarrow 2_{11}$ of R(1) [$R_{211}(1)$], $2_{12} \rightarrow 2_{11}$ of Q(2) [$Q_{211}(2)$], $1_{11} \rightarrow 2_{12}$ of R(1) [$R_{212}(1)$], $2_{11} \rightarrow 2_{12}$ of Q(2) [$Q_{212}(2)$], $2_{02} \rightarrow 3_{03}$ of R(2) [$R_{303}(2)$], $2_{11} \rightarrow 3_{12}$ of R(2) [$R_{312}(2)$], and $2_{12} \rightarrow 3_{13}$ of R(2) [$R_{313}(2)$], were chosen for the selection of the rotational levels, $N'_{K_a'K_c'} = 0_{00}$, 1_{01}, 1_{10}, 1_{11}, 2_{02}, 2_{11}, 2_{12}, 3_{03}, 3_{12}, and 3_{13}, respectively, of the υ_{11} intermediate vibrational state. We note that we have obtained previously similar IR−VUV−PFI-PE spectra by using the low-resolution IR-OPO laser to excite the P(1), P(2), R(1), and R(2) lines for the preparation of the respective $N' = 0$, 1, 2, and 3 rotational levels of $C_2H_4(\upsilon_{11})$. As shown in the comparison of Figure 1a,b, the P(2), R(1), and R(2) lines thus selected comprises of three unresolved rotational transitions.

TABLE 2: Relative Rotationally Resolved State-to-State Photoionization Cross Sections for the $\upsilon_{11} \rightarrow \upsilon_2^+ + \upsilon_{12}^+$ Vibrational Band of $C_2H_4^+$

IR transitions[a] $N''_{Ka''Kc''} \rightarrow N'_{Ka'Kc'}$	VUV transitions[b] $N'_{Ka'Kc'} \rightarrow N^+_{Ka+'Kc+}$	$\sigma(N'_{Ka'Kc'} \rightarrow N^+_{Ka+'Kc+})$[c]
$P_{000}(1)$: $1_{01} \rightarrow 0_{00}$	$0_{00} \rightarrow 1_{10}$	3.8
	$0_{00} \rightarrow 2_{12}$	1.0
	$0_{00} \rightarrow 3_{12}$	1.6
$P_{101}(2)$: $2_{02} \rightarrow 1_{01}$	$1_{01} \rightarrow 1_{11}$	2.3
$R_{101}(0)$: $0_{00} \rightarrow 1_{01}$	$1_{01} \rightarrow 2_{11}$	2.6
	$1_{01} \rightarrow 3_{13}$	1.2
	$1_{01} \rightarrow 4_{13}$	1.7
$P_{110}(2)$: $2_{11} \rightarrow 1_{10}$	$1_{10} \rightarrow 0_{00}$	5.8
$Q_{110}(1)$: $1_{11} \rightarrow 1_{10}$	$1_{10} \rightarrow 2_{02}$	5.6
	$1_{10} \rightarrow 4_{04}$	2.1
	$1_{10} \rightarrow 2_{20}$	2.8
	$1_{10} \rightarrow 3_{22}$	0.6
$Q_{111}(1)$: $1_{10} \rightarrow 1_{11}$	$1_{11} \rightarrow 1_{01}$	6.9
$P_{111}(2)$: $2_{12} \rightarrow 1_{11}$	$1_{11} \rightarrow 3_{03}$	2.6
	$1_{11} \rightarrow 2_{21}$	3.4
	$1_{11} \rightarrow 3_{21}$	0.4
$R_{202}(1)$: $1_{01} \rightarrow 2_{02}$	$2_{02} \rightarrow 1_{01}$	2.4
	$2_{02} \rightarrow 2_{12}$	1.8
	$2_{02} \rightarrow 3_{12}$	2.0
	$2_{02} \rightarrow 4_{14}$	0.8
	$2_{02} \rightarrow 5_{15}$	1.4
$Q_{211}(2)$: $2_{12} \rightarrow 2_{11}$	$2_{11} \rightarrow 1_{01}$	4.3
$R_{211}(1)$: $1_{10} \rightarrow 2_{11}$	$2_{11} \rightarrow 3_{03}$	3.4
	$2_{11} \rightarrow 2_{21}$	1.1
	$2_{11} \rightarrow 3_{21}$	1.2
$Q_{212}(2)$: $2_{11} \rightarrow 2_{12}$	$2_{12} \rightarrow 0_{00}$	1.8
$R_{212}(1)$: $1_{11} \rightarrow 2_{12}$	$2_{12} \rightarrow 2_{02}$	10.0
	$2_{12} \rightarrow 4_{04}$	3.9
	$2_{12} \rightarrow 2_{20}$	1.1
	$2_{12} \rightarrow 3_{22}$	1.9
$R_{303}(2)$: $2_{02} \rightarrow 3_{03}$	$3_{03} \rightarrow 1_{11}$	2.7
	$3_{03} \rightarrow 2_{11}$	3.1
	$3_{03} \rightarrow 3_{13}$	3.5
	$3_{03} \rightarrow 4_{13}$	3.3
	$3_{03} \rightarrow 5_{15}$	2.1
	$3_{03} \rightarrow 6_{15}$	1.5
$R_{312}(2)$: $2_{11} \rightarrow 3_{12}$	$3_{12} \rightarrow 0_{00}$	0.5
	$3_{12} \rightarrow 2_{02}$	2.1
	$3_{12} \rightarrow 4_{04}$	1.6
	$3_{12} \rightarrow 2_{20}$	1.1
	$3_{12} \rightarrow 3_{22}$	0.5
	$3_{12} \rightarrow 6_{06}$	1.1
$R_{313}(2)$: $2_{12} \rightarrow 3_{13}$	$3_{13} \rightarrow 1_{01}$	0.5
	$3_{13} \rightarrow 3_{03}$	2.9
	$3_{13} \rightarrow 2_{21}$	0.5
	$3_{13} \rightarrow 3_{21}$	2.0

[a] IR excitation transitions for the preparation of C_2H_4 in selected rovibrational levels (υ_{11}, $N'_{Ka'Kc'}$). [b] VUV photoionization transitions from selected rovibrational levels $C_2H_4(\upsilon_{11}, N'_{Ka'Kc'})$ to $C_2H_4^+(\upsilon_2^+ + \upsilon_{12}^+, N^+_{Ka+'Kc+})$. [c] Relative cross sections for the state-to-state photoionization transitions: $C_2H_4(\upsilon_{11}, N'_{Ka'Kc'}) \rightarrow C_2H_4^+(\upsilon_2^+ + \upsilon_{12}^+, N^+_{Ka+'Kc+})$. Here, the highest cross section $\sigma(2_{12} \rightarrow 2_{02})$ has been arbitrarily normalized to 10.

The IR−VUV−PFI-PE spectra (lower and middle spectra) obtained in this study with $C_2H_4(\upsilon_{11})$ prepared in individual $N'_{K_a'K_c'} = (1_{01}, 1_{10}$, and $1_{11})$, $(2_{02}, 2_{11}$, and $2_{12})$, and $(3_{03}, 3_{12}$, and $3_{13})$ rotational levels are plotted in Figure 3 a1−c1, a2−c2, and a3−c3. The upper spectra marked as sim shown in Figure 3a1−c1, a2−c2, and a3−c3 are simulated spectra. The PFI-PE intensities [I(PFI-PE)] of all the figures have been normalized by the VUV intensity [$I(h\nu)$]. To show the relative intensities for the rotational transitions, the vertical scales of these spectra have the same I(PFI-PE)/$I(h\nu)$ units. The assignments of rotational transitions are also marked on top of these

figures. Almost all the observed rotational patterns match the predicted rotational transitions based on the selection rules, except for the $Q_{111}(1)$ spectrum of Figure 3c1 and the $Q_{211}(2)$ and $R_{211}(1)$ spectra of Figure 3c2, where a shoulder peak to the red of the respective transition lines $1_{11} \rightarrow 2_{21}$ and $2_{11} \rightarrow 2_{21}$ cannot be assigned. We note that the $N'_{K_a'K_c'} = 1_{01}$, 1_{10}, 1_{11}, 2_{11}, and 2_{12} levels can be prepared by two IR transitions, namely, $P_{101}(2)$ and $R_{101}(0)$, $P_{110}(2)$ and $Q_{110}(1)$, $Q_{111}(1)$ and $P_{111}(2)$, $Q_{211}(2)$ and $R_{211}(1)$, and $Q_{212}(2)$ and $R_{212}(1)$, respectively. As shown in Figure 3 a1, b1, c1, b2, and c2, the rotational structures observed by employing the two transition schemes are in agreement after taking into account of the experimental uncertainties. The rotational structure resolved in the IR−VUV−PFI-PE spectrum for $N' = 0$ reported previously is consistent with that for $N'_{K_a'K_c'} = 0_{00}$ observed in the present study because the P(1) line only consists of the single $1_{01} \rightarrow 0_{00}$ transition. For this reason, the IR−VUV−PFI-PE spectrum for $N'_{K_a'K_c'} = 0_{00}$ is not shown here.

Table 2 summarizes the IR transitions $N''_{K_a''K_c''} \rightarrow N'_{K_a'K_c'}$ for the preparation of the $N'_{K_a'K_c'} = 0_{00}$, 1_{01}, 1_{10}, 1_{11}, 2_{02}, 2_{11}, 2_{12}, 3_{03}, 3_{12}, and 3_{13} levels and the VUV photoionization transitions $N'_{K_a'K_c'} \rightarrow N^+_{K_a+'K_c+}$ resolved in the present IR−VUV−PFI-PE measurements. The relative cross sections $[\sigma(N'_{K_a'K_c'} \rightarrow N^+_{K_a+'K_c+})]$ for the photoionization transitions $(\upsilon_{11}, N'_{K_a'K_c'}) \rightarrow (2\upsilon_4^+ + \upsilon_{12}^+, N^+_{K_a+'K_c+})$ are determined on the basis of the measured relative intensities of the rotational lines resolved in Figure 3 a1−c1, a2−c2, and a3−c3 and have been normalized by the relative intensities of the selected IR transitions for the preparation of the $(\upsilon_{11}, N'_{K_a'K_c'})$ levels as determined in Figure 1a. The $\sigma(N'_{K_a'K_c'} \rightarrow N^+_{K_a+'K_c+})$ values of Table 2 are obtained by arbitrarily normalizing the cross section of the strongest transition line $2_{12} \rightarrow 2_{02}$ to be $\sigma(2_{12} \rightarrow 2_{02}) = 10$. The $\sigma(N'_{K_a'K_c'} \rightarrow N^+_{K_a+'K_c+})$ values associated with the $N'_{K_a'K_c'} = 1_{01}$, 1_{10}, 2_{11}, and 2_{12}, levels represent the average of two sets of measurements obtained by the two rotational transition schemes for the preparation of these levels. Due to the poor signal-to-noise ratios of the cross section values obtained via the $P_{111}(2)$ transition, they are not included in the determination of the cross section values for $N'_{K_a'K_c'} = 1_{11}$ given in Table 2. The determination of the $\sigma(N'_{K_a'K_c'} \rightarrow N^+_{K_a+'K_c+})$ values requires the measurement of the relative populations of the selected $N'_{K_a'K_c'}$ rotational levels, which are estimated by the relative IR−VUV−PI intensities of the $N''_{K_a''K_c''} \rightarrow N'_{K_a'K_c'}$ transitions. The populations for the $N'_{K_a'K_c'}$ rotational levels determined by the IR−VUV−PI measurement are subject to some uncertainties. Thus, the $\sigma(N'_{K_a'K_c'} \rightarrow N^+_{K_a+'K_c+})$ values given in Table 2 should be viewed as crude estimates. Nevertheless, the trend of these cross sections should be reliable. As shown in Table 2, the most intense peaks correspond to $\Delta N^+ = 0$ and ± 1, indicating that photoionization favors small changes in the rotational angular momentum or the angular momentum of the photoelectron. The maximum change of $\Delta N^+ = 3$ has been observed in most of the spectra, which corresponds to a *d* partial wave for the departing photoelectron. Furthermore, the high $\sigma(N'_{K_a'K_c'} \rightarrow N^+_{K_a+'K_c+})$ values are found to favor the formation of the ions in the lowest $N^+_{K_a+'K_c+}$ rotational levels with $K_a^+ = 0$.

V. Conclusions

The use of a single mode IR-OPO laser has enabled the complete resolution of the rotational structure and the selection of single rotational levels of $C_2H_4(\upsilon_{11})$ for VUV−PFI-PE measurements. The IR−VUV−PFI-PE measurement of $C_2H_4(\upsilon_{11}, N'_{K_a'K_c'} = 3_{03})$ revealed detailed rovibrational structures of $C_2H_4^+(\tilde{X}^2B_{3u})$, allowing the observation of 14 new ion vibrational bands in the range of 1200−3000 cm^{-1} above the IE-(C_2H_4). The frequencies of these new vibrational bands have made possible the determination of the fundamental vibrational frequencies for $\upsilon_8^+ = 1103 \pm 10$ and $\upsilon_{10}^+ = 813 \pm 10$ cm^{-1}. We have also examined the rotationally resolved IR−VUV−PFI-PE spectra for the $(\upsilon_{11}; N'_{K_a'K_c'}) \rightarrow (\upsilon_2^+ + \upsilon_{12}^+)$ band by selecting $N'_{K_a'K_c'} = 0_{00}$, 1_{01}, 1_{10}, 2_{02}, 2_{11}, 2_{12}, 3_{03}, 3_{12}, and 3_{13} states. The relative rovibrationally resolved state-to-state photoionization cross sections should be useful for benchmarking state-of-the-art theoretical calculations on photoionization dynamics. This experiment has demonstrated that the two-color IR−VUV−PI and IR−VUV−PFI-PE methods are sensitive high-resolution techniques for spectroscopic studies of neutrals and ions.

Acknowledgment. This work is supported by the NSF Grant No. CHE 0517871. We also acknowledge partial supports by the DOE Grant No. DE-FG02-02ER15306, the AFOSR Grant No. FA9550-06-1-0073, and the NASA Grant No. 07-PATM07-0012. The calculations were performed using the National Energy Research Scientific Computing Center and the Molecular Science Computing Facility supported by DOE.

References and Notes

(1) Smalley, R. E.; Ramakrishna, B. L.; Levy, D. H.; Wharton, L. *J. Chem. Phys.* **1974**, *61*, 4363.

(2) Ng, C. Y. *Annu. Rev. Phys. Chem.* **2002**, *53*, 101−140.

(3) Powis, I., Baer, T., Ng, C. Y., Eds. *High Resolution Laser Photoionization and Photoelectron Studies*; Wiley Series in Ion Chemisty & Physics; Wiley: Chichester, U.K., 1995.

(4) Qian, X.-M.; Kung, A. H.; Zhang, T.; Lau, K. C.; Ng, C. Y. *Phys. Rev. Lett.* **2003**, *91*, 233001.

(5) Woo, H. K.; Wang, P.; Lau, K.-C.; Xing, X.; Chang, C.; Ng, C. Y. *J. Chem. Phys.* **2003**, *119*, 9333−9336.

(6) Wang, P.; Xing, X.; Lau, K.-C.; Woo, H. K.; Ng, C. Y. *J. Chem. Phys.* **2004**, *121*, 7049.

(7) Wang, P.; Xing, X.; Baek, S. J.; Ng, C. Y. *J. Phys. Chem. A* **2004**, *108*, 10035.

(8) Xing, Xi; Bahng, M.-K.; Wang, P.; Lau, K. C.; Baek, S.-J.; Ng, C. Y. *J. Chem. Phys.* **2006**, *125*, 133304 and references therein.

(9) Willitsch, S.; Hollenstein, U.; Merkt, F. *J. Chem. Phys*. **2004**, *120*, 1761.

(10) Xing, X.; Reed, B.; Lau, K.-C.; Baek, Sun-Jong; Bahng, Mi-Kyung; Ng, C. Y. *J. Chem. Phys.* **2007**, *127*, 044313.

(11) Woo, H. K.; Lau, K.-C.; Zhan, J. P.; Ng, C. Y.; Cheung, Y. S.; Li, W. K.; Johnson, P. M. *J. Chem. Phys*. **2003**, *119*, 7789.

(12) Bahng, Mi-Kyung; Xing, Xi; Jong Baek, Sun; Ng, C. Y. *J. Chem. Phys.* **2005**, *123*, 084311.

(13) Legrand, J.; Azizi, A.; Herlemont, F.; Fayt, A. *J. Mol. Spectrosc.* **1995**, *171*, 13.

(14) Bach, M.; Georges, R.; Hepp, M.; Herman, M. *Chem. Phys. Lett.* **1998**, *294*, 533.

(15) Bunker, P. R.; Jensen, P. *Molecular Symmetry and Spectroscopy*, 2nd ed.; NRC Research Press: Ottawa, 1998.

(16) Martin, J. M. L.; Taylor, P. R. *Chem. Phys. Lett*. **1996**, *248*, 336.

(17) Knowles, P. J.; Hampel, C.; Werner, H. J. *J. Chem. Phys*. **1988**, *99*, 5219.